International Journal of Design & Nature and Ecodynamics
Vol. 21, No. 1, January, 2026, pp. 81-89
Journal homepage: http://iieta.org/journals/ijdne

Development and Characterization of Vitamin C-Loaded Chitosan/Alginate Microcapsules for Enhanced Oral Immunostimulation in Aquaculture

Karl Marx A. Quiazon[1], Jefferson D. Gagelonia[1*], Aries Paul D. Padron[1], Cherry Ann Kindipan[1], Kae M. Damian[1], Jefferson C. Bautista[1], Cheryl Grace B. Hoggang[1], Roberto J. Mateo Jr.[1], Paul Jhon G. Eugenio[2], Juvy J. Monserate[2], Faith S. Tadeo[3], Aphrodite S. Entoma[3], Benyl John A. Arevalo[4], Niko A. Macaraeg[5], Casiano H. Choresca Jr.[6]

[1] Freshwater Aquaculture Center, Central Luzon State University, Science City of Muñoz 3120, Philippines
[2] Department of Chemistry, Central Luzon State University, Science City of Muñoz 3120, Philippines
[3] Don Mariano Marcos Memorial State University, Agoo 2505, Philippines
[4] Bicol University Tabaco Campus, Tabaco City 4511, Philippines
[5] Department of Agriculture, National Fisheries Research and Development Institute, Quezon City 1128, Philippines
[6] Fisheries Biotechnology Center, National Fisheries Research and Development Institute, Science City of Muñoz 3120, Philippines

Corresponding Author Email: jefferson_gagelonia@clsu.edu.ph

https://doi.org/10.18280/ijdne.210108

Received: 18 November 2025
Revised: 13 January 2026
Accepted: 22 January 2026
Available online: 31 January 2026

Keywords:
aquatic animal health, biopolymer-based delivery system, drug delivery, fish immunization, immunostimulant, optimization, screening, vaccine delivery

ABSTRACT

Immunostimulants are widely used in aquaculture to enhance host immune responses and improve disease resistance. Vitamin deficiencies, by contrast, are primarily prevented or corrected through dietary vitamin supplementation. Notably, vitamin C (ascorbic acid), although a vitamin, is also frequently studied as an immunostimulant due to its immunomodulatory effects. In parallel, oral vaccination has emerged as a promising strategy for mass immunization in aquaculture because it is easy to administer, reduces handling stress, and can be cost-effective. However, harsh gastrointestinal conditions can degrade orally administered bioactives before they elicit a measurable immune response. Moreover, vitamin C is one of the most commonly utilized immunostimulants administered orally, yet its sensitivity to the environment poses a major problem during fish immunization due to leaching. Therefore, this research aimed to optimize a biopolymer-based microencapsulation system using a chitosan–alginate biopolymer system for the effective oral delivery of vitamin C as an immunostimulant in tilapia. A Box–Behnken experimental design was employed to evaluate the effects of key formulation parameters, sodium alginate concentration, vitamin C concentration, and gelling time on encapsulation efficiency (EE) and loading capacity (LC). Results showed that these variables significantly affected both %EE and %LC. The optimal formulation comprised 1.0% sodium alginate and 0.05 ppm vitamin C with immediate gelation, achieving 84.19% EE and 0.471% LC. Spectrophotometric and thermogravimetric analyses confirmed successful vitamin C encapsulation, and the optimized microcapsules exhibited uniform morphology and excellent stability. This microencapsulation strategy demonstrates strong potential for enhancing the oral delivery of vitamin C (and potentially other labile immunostimulants) in tilapia.

1. INTRODUCTION

Vitamin C is an essential micronutrient that supports innate and adaptive immunity in humans and animals and is associated with reduced stress, improved growth performance, and enhanced immune function [1]. In aquaculture, vitamin C is widely used to support fish health and immune competence and may reduce disease susceptibility and mortality under stress conditions [2]. It is commonly incorporated in fish diet and administered orally [3, 4]. However, it easily degrades when exposed to high temperatures, light, oxygen, and other environmental factors imposed during the preparation, application, and storage [5].

Immunostimulants such as vitamin C may degrade in the gastrointestinal tract and interact with feed components, substantially reducing their efficacy [6-8]. A key issue is the need to protect it until it reaches the lower gut intact, where it can elicit an immune response [3, 9, 10]. One practical approach is to use a carrier that facilitates passage through the acidic stomach and enables controlled release and absorption in the intestine. Therefore, microencapsulating the vitamin C will increase its immunostimulatory effect in Tilapia. Microencapsulation is the process of enclosing compounds in an immiscible layer to protect it from degradation until it reaches the target site with the use of biopolymers [11, 12]. Biopolymers such as chitosan and alginate have been widely

used for the delivery of bioactive compounds to help prevent or control infectious diseases [13, 14]. Recently, microcapsules have been explored as a suitable method for delivering active compounds to enhance the immunogenicity of oral vaccine antigens [15].

Chitosan and alginate are among the most commonly used polymers for encapsulation because they are biocompatible, low in toxicity, and derived from natural sources, which makes them suitable carriers for immunostimulants in animals [16]. Despite these advantages, the amount of each component used in the encapsulation process must be carefully controlled. Small changes in concentration can influence capsule stability, loading efficiency, and the release behavior of the active compounds [17]. Without proper optimization, the performance of the microcapsules may be reduced [17].

For this reason, identifying the ideal formulation requires the use of systematic experimental design methods, such as the Box–Behnken design (BBD) [18], which allows the effects of different variables to be evaluated efficiently. In this study, chitosan–alginate microcapsules were optimized to load and protect vitamin C for oral delivery, providing a basis for improving immune support in tilapia.

2. METHODOLOGY

2.1 Preparation of microcapsules

Chitosan and alginate microcapsules are the most used encapsulating agents in aquaculture as it efficiently encapsulates active compounds with high efficiency [17]. These biopolymers were prepared using the ionic gelation technique and polyelectrolyte complex formation combined with the dripping extrusion method [19-21]; employing optimized reagent concentrations of 0.5% chitosan (w/v), 1.0% (w/v) sodium alginate, 2.0% (v/v) glacial acetic acid, 4.0% (w/v) calcium chloride ($CaCl_2$), and 0.005% (w/v) L-ascorbic acid (vitamin C). These concentrations were identified by applying the optimization criteria BBD shown in Table 1.

Table 1. Optimization criteria for Box–Behnken design

Factor	Symbol	Low (−1)	Mid (0)	High (+1)	Unit
Alginate concentration	A	0.7	1.1	1.5	%
Vitamin C	B	20.0	40.0	60.0	ppm
Gelling time	C	0.0	30.0	60.0	min

Two aqueous solutions were prepared: Solution A consisted of 1.0% sodium alginate and 0.005% vitamin C dissolved in distilled water under constant stirring, while Solution B contained 0.5% chitosan dissolved in 2.0% glacial acetic acid with distilled water, to which 4.0% $CaCl_2$ was subsequently added to facilitate cross-linking and capsule formation.

Using a 10 mL syringe (19-gauge), Solution A was extruded dropwise into Solution B under gentle magnetic stirring to prevent aggregation. Upon contact, ionotropic gelation occurred, resulting in the immediate formation of chitosan–alginate capsules. The gelation period was optimized to ensure uniformity in capsule morphology and stability. The gelation period is the total time for the microcapsules to enter a solid state from their liquid state submerged in the gelling solution [22]. Different times were assigned to each trial to determine the ideal time to attain solid capsules with high EE and LC.

Following gelation, the resultant microcapsules were carefully separated and rinsed with distilled water for 5 minutes to remove any unencapsulated active compound and excess $CaCl_2$ adhered to the surface. Resultant microcapsules were then air-dried for 3–5 days at ambient temperature. The drying process significantly reduced the capsule size by approximately 90%, yielding microscale particles suitable for subsequent analysis.

2.2 Calibration curve

A stock standard solution of vitamin C (200 ppm) was prepared by dissolving 0.5 g of crystalline L-ascorbic acid (99% purity) in distilled water and diluting to a final volume of 500 mL. From this stock, a series of working standard solutions (10–100 ppm) was obtained by appropriate dilution using distilled water.

Each standard solution (4.0 mL) was transferred into a quartz cuvette and scanned using a UV–Vis spectrophotometer (Hitachi 5100 UV–Vis) to determine the maximum absorbance wavelength (λmax) of ascorbic acid. The peak wavelength was established following repeated spectral measurements. Once λmax was identified, all standard solutions were measured at this wavelength.

A calibration curve was constructed by plotting absorbance against concentration (ppm). Linear regression analysis yielded the equation:

$$y = mx + b \quad (1)$$

where, y represents absorbance, m is the change in absorbance with response to concentration (sensitivity of the method), x represents the concentration of vitamin C, and b is the background absorbance or the instrument baseline. This calibration curve was subsequently employed to determine the vitamin C content in microencapsulated immunostimulant samples. Standardization of ascorbic acid is essential to obtain reliable peak absorbance data and to ensure accurate quantitative analysis in subsequent microencapsulation studies [23].

2.3 Evaluation of encapsulation efficiency and loading capacity of microencapsulated Imm-MC

The encapsulation efficiency (EE) is the amount of active compound entrapped in the microcapsule [24]. While loading capacity (LC) is the total weight of active compound inside the microcapsule in relation to the relative weight of the whole microcapsules including the biopolymers and other materials [25]. %EE is also defined as the concentration of the incorporated material such as active ingredients, drugs, proteins, antimicrobial ingredients and such, detected in the formulation over the initial concentration used to make the formulation, whereas, LC is defined as the amount of loaded material per unit weight of micro-/nanoparticles, indicating the mass of the particle that is due to encapsulated material [26, 27].

The immunostimulants were separated from aqueous suspension by centrifugation. The supernatant was collected, and the immunostimulants were linearly detected using a UV-Vis spectrophotometer and compared to the standard curve prepared previously. The total amount of immunostimulant-loaded microcapsules (Imm-MC) incubated in the solution before the cross-linking process was also measured for further

analysis. The %EE and %LC of Imm-MC were calculated using equations:

$$\%EE = \frac{Total\ Imm\ munostimulant - Free\ Imm\ munostimulant}{Total\ Imm\ munostimulant} \times 100 \quad (2)$$

$$\%LC = \frac{Total\ Imm\ munostimulant - Free\ Imm\ munostimulant}{Total_{microcapsule(grams)}} \times 100 \quad (3)$$

2.4 Experimental design and statistical analysis

Box–Behnken design, a type of response surface methodology (RSM), was employed in the protocol to maximize %EE and %LC. Several factors, such as sodium alginate concentration (% w/v), dripping distance (ft), gelling time (min) [28], chitosan concentration, calcium chloride ($CaCl_2$) concentration (% w/v) [29], and L-ascorbic acid concentration (% w/v) [30], were screened to determine the variable that affects the encapsulation process.

Statistical analysis was performed using Design-Expert® software (version 13.0, Stat-Ease Inc., Minneapolis, MN, USA). The software was used to generate the randomized experimental matrix, model the response surfaces, and determine optimal process conditions through analysis of variance (ANOVA), 3D response surface plots, and desirability function-based multi-response optimization.

3. RESULTS AND DISCUSSIONS

3.1 Vitamin C standardization and calibration curve

A series of wavelength scans identified the peak absorbance of vitamin C at 261 nm, which closely aligns with the value (i.e., 264 nm) reported by Harvey and Palumbo [31]. The wavelength found at 261 nm was found in several concentrations as well as in the stock solution. The absorbance peak of vitamin C at 261 nm lies in the UV region due to $\pi \rightarrow \pi^*$ electronic transitions within its conjugated enediol – lactone system. The UV light provides just the right amount of energy to excite π-electrons in this conjugated structure, leading to a strong absorbance band near 261 nm. This behavior is consistent with known values (e.g., 264 nm) and is characteristic of colorless organic molecules with conjugated carbonyl and hydroxyl groups. This wavelength was subsequently used for all absorbance measurements (Table 2).

Table 2. The average absorbance reading of each vitamin C concentration under the UV-Vis spectrophotometer

Vitamin C (ppm)	Average Absorbance (nm)
10	0.831
20	1.093
30	1.460
40	1.791
50	2.100
60	2.777
70	2.600
80	2.900
90	3.242
100	3.345

A strong linear relationship was observed on the calibration curve plotted by graphing absorbance values against vitamin C concentrations. The linear regression equation derived from this dataset was:

$$y = 0.0042x + 0.0481 \quad (4)$$

The coefficient of determination was $R^2 = 0.9824$. This high coefficient of determination ($R^2 < 1$) indicates strong linearity and minimal deviation, validating the model for predicting unknown concentrations of vitamin C in microencapsulated samples [32]. The standard curve (Figure 1) was used throughout this research to determine %EE and %LC, thereby supporting quantitative assessments of the microcapsule formulations.

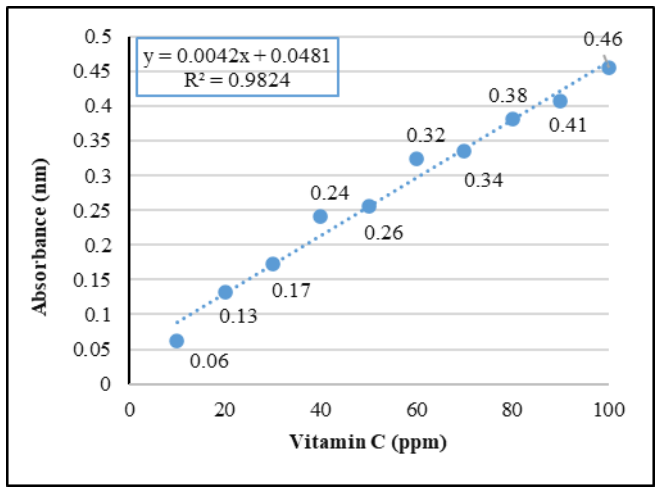

Figure 1. The calibration curve of vitamin C

The generated linear regression equation (y = 0.0042x + 0.0481, R^2 = 0.9824) was subsequently used for the quantitative determination of vitamin C concentration in samples before and after encapsulation. This enabled the calculation of %EE and %LC. The same equation was also applied in subsequent analyses involving vitamin C quantification, ensuring consistency and reliability of results throughout the research.

3.2 Screening and optimization

The effects of alginate concentration (A), vitamin C concentration (B), and gelling time (C) on EE and LC were evaluated using a Box–Behnken design. The observed responses are summarized in Table 3.

EE varied widely from 30.13% to 83.21%, indicating that formulation parameters strongly influenced microcapsule performance. Low EE values were primarily observed in formulations containing 20 ppm vitamin C, particularly at short (0 min) or intermediate (30 min) gelling times, irrespective of alginate concentration. In contrast, formulations with 60 ppm vitamin C generally exhibited higher EE, with the maximum value (83.21%) achieved at 0.7% alginate concentration, 60 ppm vitamin C, and 30 min gelling time. This trend reflects the importance of vitamin C availability in the entrapment process, where insufficient concentration reduces payload incorporation, while excess may approach the retention capacity of the polymer matrix, leading to diffusion losses [33].

LC ranged from 0.09% to 0.47% and followed a trend similar to EE. The highest LC (0.47%) corresponded to the same formulation that produced the maximum EE. Formulations containing 1.5% alginate and 20 ppm vitamin C resulted in the lowest LC values, likely due to high polymer content limiting space for active compound incorporation and

low vitamin C concentration reducing payload availability [34]. Center-point replicates (1.1% alginate, 40 ppm vitamin C, 30 min gelling time) yielded consistent EE and LC values, demonstrating reproducibility and low experimental error.

Table 3. Box–Behnken experimental design showing the levels of alginate concentration, vitamin C concentration, and gelling time, with the corresponding encapsulation efficiency (EE) and loading capacity (LC)

Factor 1	Factor 2	Factor 3	Response 1	Response 2
A: Alg. Conc	B: Vit. C	C: Gelling Time	EE	LC
%	ppm	min	%	%
1.1	40	30	74.14	0.29
1.5	60	30	74.13	0.23
1.5	40	0	73.51	0.25
1.5	60	30	77.28	0.24
1.1	40	30	74.46	0.26
1.1	20	0	36.85	0.16
0.7	40	0	76.09	0.4
1.5	20	30	35.48	0.09
1.1	40	30	69.71	0.19
1.1	40	30	70.31	0.16
1.1	40	30	73.14	0.27
0.7	60	30	83.21	0.42
1.1	60	0	81.28	0.35
1.1	20	60	37.99	0.13
1.5	40	60	67.48	0.18
0.7	40	60	74.8	0.29
0.7	40	60	77.29	0.25
1.1	40	30	70.91	0.22
1.1	60	60	75.79	0.09
1.1	60	0	80.77	0.29
1.1	20	0	30.22	0.1
0.7	60	30	81.27	0.47
1.5	40	60	69.52	0.17
0.7	40	0	73.02	0.38
1.5	40	0	68.49	0.18
0.7	20	30	34.12	0.14
0.7	20	30	30.13	0.14
1.1	60	60	80.59	0.23
1.1	20	60	38.03	0.1
1.5	20	30	35.13	0.09

Overall, vitamin C concentration emerged as the most influential factor affecting both EE and LC, followed by alginate concentration, while gelling time exhibited a secondary but interactive effect. These observations are consistent with previous reports indicating that hydrophilic small molecules are sensitive to both polymer matrix density and exposure time during ionic gelation [35, 36].

3.2.1 Regression model and coefficient interpretation

The responses (%EE and %LC) were influenced significantly by alginate concentration, vitamin C concentration, and gelling time, with notable interaction and quadratic effects (Tables 4 and 5). ANOVA results confirmed the models were statistically significant, with high F-values and p-values < 0.05 for critical terms, while lack-of-fit tests were non-significant, indicating the models adequately describe the observed experimental variation [37].

For EE, the regression model indicated that increasing alginate and vitamin C concentrations generally enhanced EE, while gelling time had a smaller positive or neutral effect. Negative interaction terms suggest that simultaneous increases in certain factors beyond optimal levels could slightly reduce EE, consistent with a balance between polymer density and payload diffusion. The quadratic term for alginate (A^2) revealed a pronounced curvature, indicating that EE initially rises with alginate concentration but may decrease if the polymer network becomes overly dense, limiting vitamin C incorporation [38].

Table 4. ANOVA results for encapsulation efficiency (EE) showing the significance of model terms, including main factors, interactions, and quadratic effects

Source	Sum of Squares	Mean Square	F-Value	p-Value
Model	9818.68	1636.45	297.06	< 0.0001**
A-Alg. Conc	52.24	52.24	9.48	0.0053**
B-Vit. C	7937.47	7937.47	1440.87	< 0.0001**
C-Gelling Time	0.0992	0.0992	0.0180	0.8944^{ns}
AB	47.19	47.19	8.57	0.0076**
BC	26.72	26.72	4.85	0.0379**
B^2	1754.96	1754.96	318.57	< 0.0001**
Residual	126.70	5.51		
Lack of Fit	34.57	5.76	1.06	0.4216^{ns}
Pure Error	92.13	5.42		
Cor Total	9945.38			

Note: ** = significant and ns = not significant.

Table 5. ANOVA results for loading capacity (LC), indicating the contribution of main factors, interactions, and quadratic effects to the response

Source	Sum of Squares	Mean Square	F-Value	p-Value
Model	0.2653	0.0379	17.89	< 0.0001**
A-Alg. Conc	0.0702	0.0702	33.15	< 0.0001**
B-Vit. C	0.1173	0.1173	55.37	< 0.0001**
C-Gelling Time	0.0281	0.0281	13.24	0.0014**
AB	0.0128	0.0128	6.04	0.0223**
BC	0.0105	0.0105	4.96	0.0365**
A^2	0.0114	0.0114	5.37	0.0302**
B^2	0.0132	0.0132	6.22	0.0206**
Residual	0.0466	0.0021		
Lack of Fit	0.0153	0.0031	1.66	0.1987^{ns}
Pure Error	0.0313	0.0018		
Cor Total	0.3119			

Note: ** = significant and ns = not significant.

The LC model revealed that alginate concentration exerted a strong negative linear effect and a positive quadratic effect, highlighting an optimal polymer concentration for maximum LC. Vitamin C and gelling time contributed modestly to LC, mainly fine-tuning payload incorporation without major influence on overall behavior.

3.2.2 Residual and model validation

Normal probability plots of residuals for EE and LC indicated approximate normal distribution, confirming the validity of ANOVA assumptions T. Residuals versus run plots demonstrated randomness and independence, with no visible systematic trends or outliers, supporting the adequacy and reliability of the developed regression models (Figures 2-3). These findings confirm that the selected design and model terms effectively capture the relationships between formulation parameters and microcapsule performance.

The residuals versus run plots for %EE and %LC (Figure 3) were analyzed to examine the randomness and independence of the residuals across experimental runs (Figure 3). For both responses, the residuals were randomly scattered around the horizontal zero line, with no visible systematic trends or cyclical patterns. This random distribution indicates that the

experimental errors were independent and not influenced by the sequence of runs or any time-related factors [39]. Additionally, all data points fell within the control limits (± 3.6595), confirming the absence of outliers or influential observations. The color-coded residuals, representing varying %EE (30.13–83.21) and LC (0.09–0.47) values, were evenly distributed without any noticeable clustering or bias. These findings further validate the adequacy and stability of the developed regression models, demonstrating that the model predictions are reliable and free from systematic experimental errors.

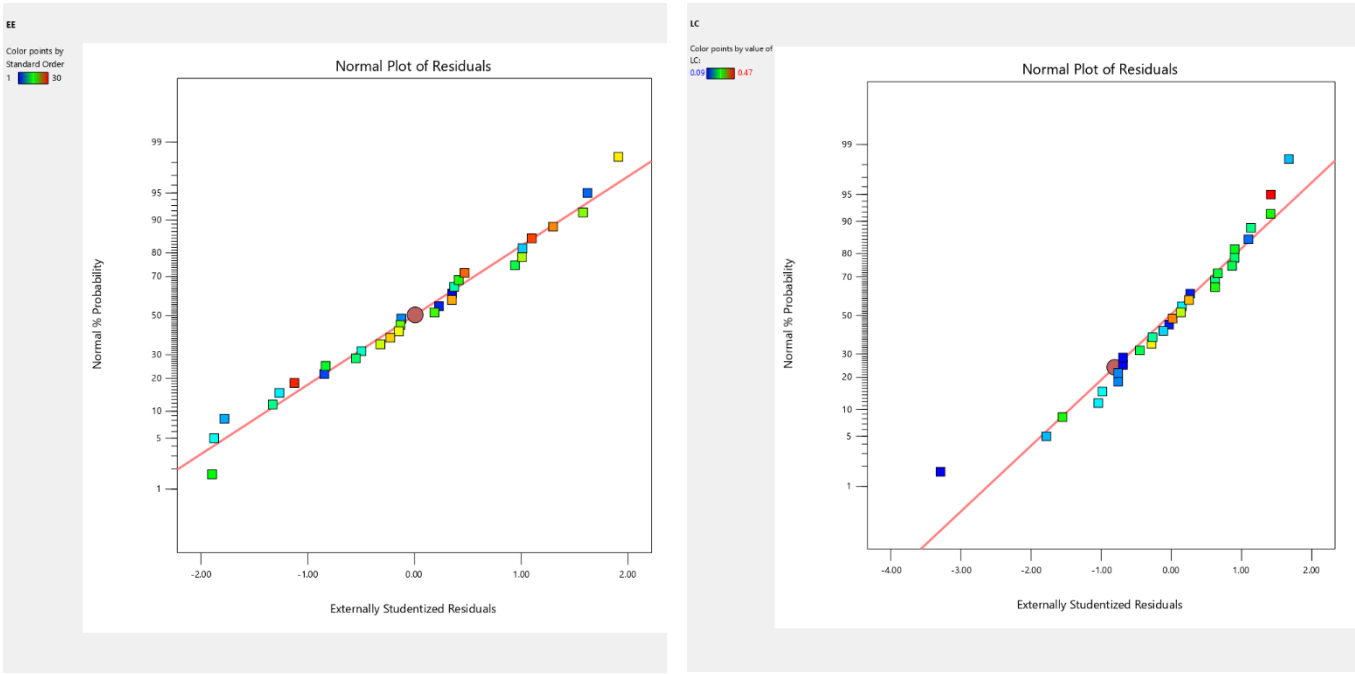

(a) Normal probability plot of residuals of EE

(b) Normal probability plot of residuals of LC

Figure 2. Normal probability plots of residuals for (a) encapsulation efficiency (EE) and (b) loading capacity (LC), demonstrating approximate normal distribution of residuals and validating model assumptions

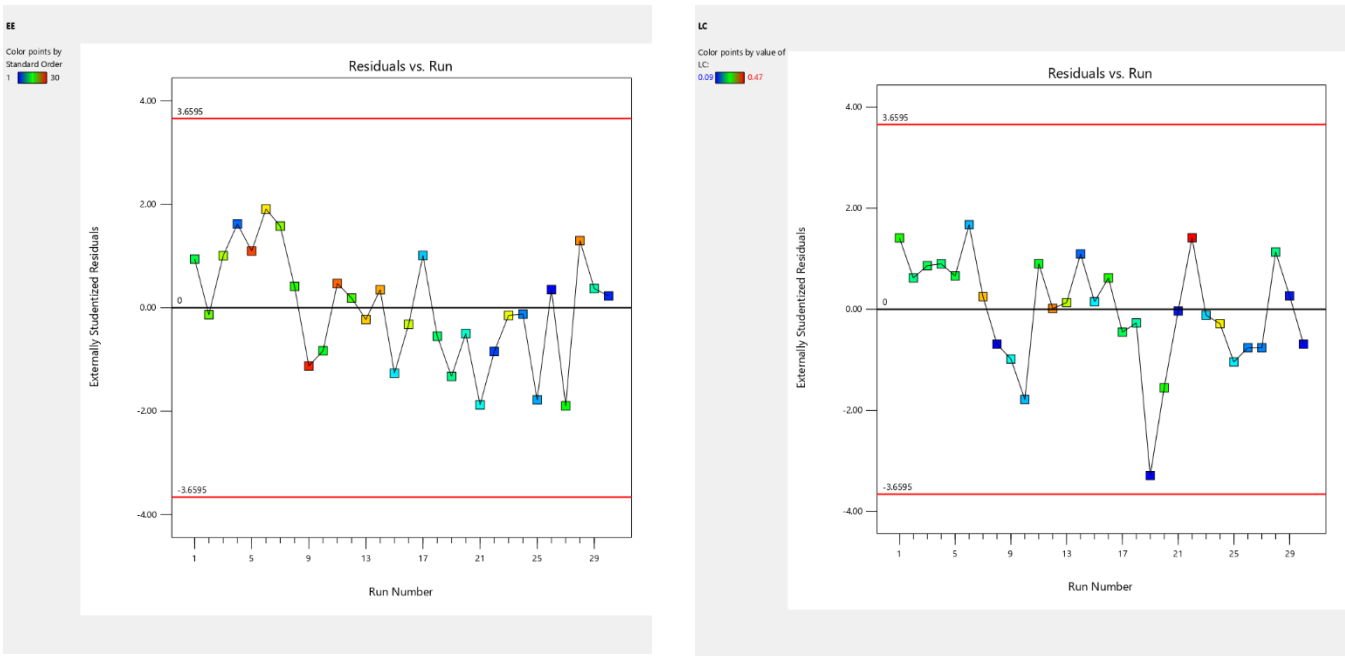

(a) Residuals versus run plots for %EE

(b) Residuals versus run plots for %LC

Figure 3. Residuals versus run plots for (a) EE and (b) LC
Random scatter around the zero line indicates independence of experimental errors and absence of systematic bias or outliers.

3.2.3 3D surface response analysis

Three-dimensional surface plots illustrated the combined effects of alginate and vitamin C concentrations on EE and LC. EE increased with both variables, reaching maximum values at elevated levels due to enhanced polymer network cohesion and stronger crosslinking [40]. Conversely, LC decreased under the same conditions due to reduced internal pore space, emphasizing the need for balanced formulations to achieve optimal overall performance. The optimal formulation predicted by the model (0.766% alginate, 59.36 ppm vitamin

C, 1.81 min gelling time) yielded EE of 84.06% and LC of 0.47%, with a desirability value of 1.0, demonstrating the robustness of the optimization approach. The opposing trends between EE and LC observed in 3D surface plots (Figure 4) highlight a critical formulation trade-off: higher polymer density improves EE but reduces the fraction of payload relative to total microcapsule mass.

The residual analysis validates the adequacy, accuracy, and reliability of the regression models developed for predicting %EE and LC. The close conformity of the residuals to the normal distribution further supports that the selected experimental design and model terms were appropriate for describing the relationships between the process parameters and the measured responses.

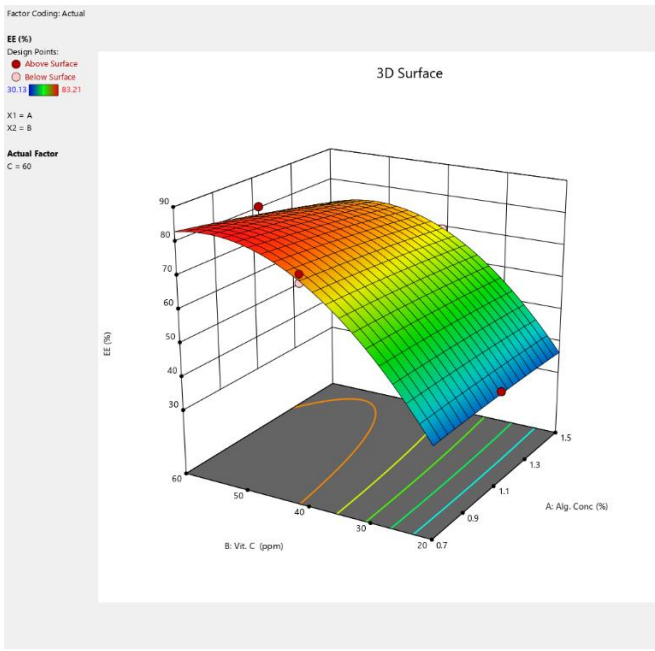

(a) Three-dimensional surface plot for EE

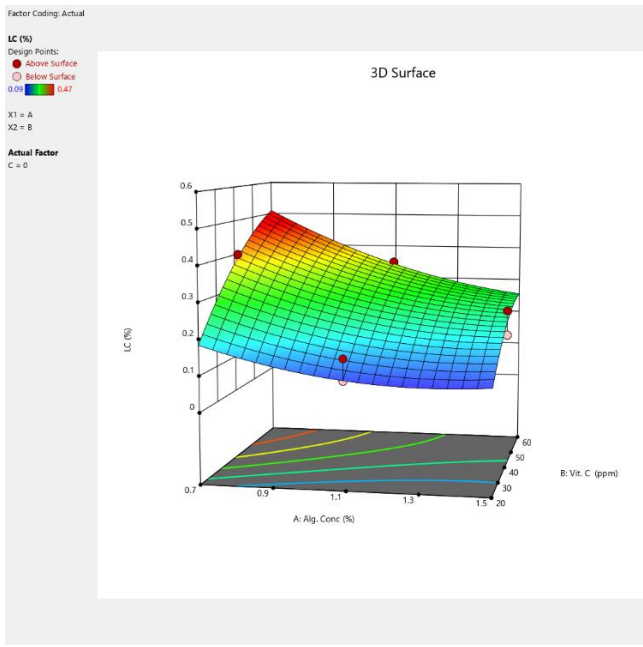

(b) Three-dimensional surface plot for LC

Figure 4. Three-dimensional surface plots illustrating the combined effects of alginate concentration and vitamin C concentration on (a) EE and (b) LC

EE increases with higher A and B, while LC decreases, highlighting a trade-off between efficiency and payload loading.

3.2.4 Characterization of microcapsule

Scanning electron microscopy (SEM) analysis (Figure 5) revealed microcapsules with compact, irregularly flattened morphology, diameters ranging from 800–1100 µm, and mostly smooth surfaces with minor cracks and wrinkles, likely resulting from dehydration during drying [41].

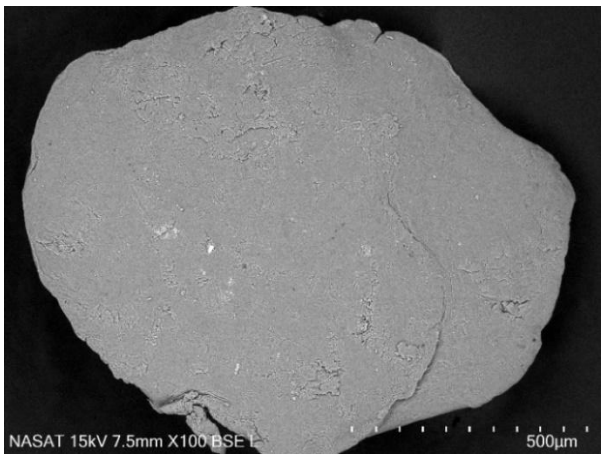

Figure 5. Scanning electron microscopy (SEM) micrograph of Imm-MC at 100× magnification

The capsules exhibit irregular, flattened morphology with smooth surfaces, minor cracks, and compact structure.

Scanning electron microscopy–energy-dispersive X-ray spectroscopy (SEM–EDS) (Figure 6) confirmed carbon and oxygen as dominant elements, consistent with alginate–chitosan polymer matrices and vitamin C incorporation, while calcium signals confirmed successful ionic crosslinking [42].

Thermogravimetric analysis (TGA) (Figure 7) showed higher mass loss for Imm-MC compared to blanks at low and intermediate temperatures, reflecting payload decomposition and moisture release. Additional degradation steps at intermediate temperatures and higher residual loss at high temperatures further confirmed successful incorporation and structural stability of the encapsulated vitamin C [34].

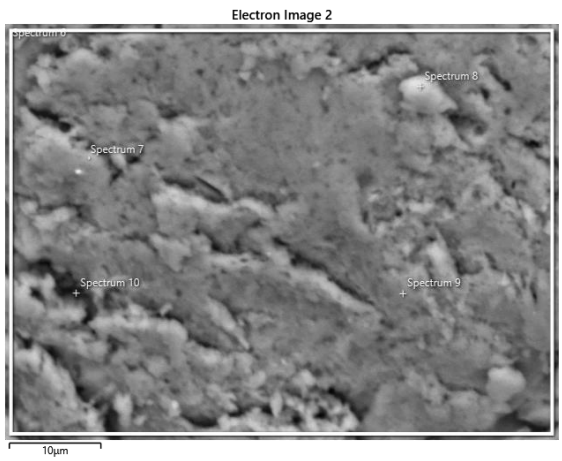

Figure 6. Scanning electron microscopy–energy-dispersive X-ray spectroscopy (SEM–EDS) elemental mapping of microcapsules

High signals of carbon and oxygen confirm polymer matrix and vitamin C incorporation, while calcium indicates successful ionic crosslinking.

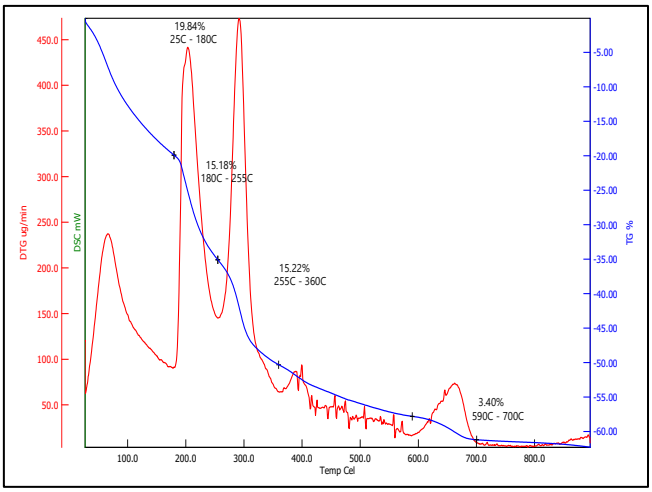

(a) Thermogravimetric data of blank microcapsules

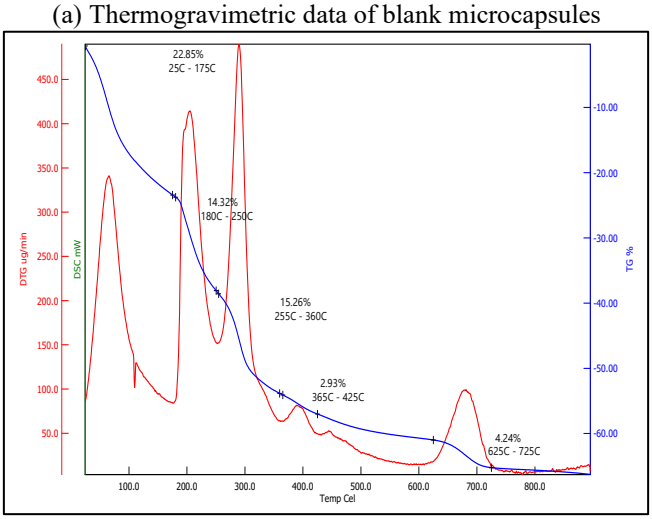

(b) Thermogravimetric data of Imm-MC microcapsules

Figure 7. Thermogravimetric analysis (TGA) and derivative thermogravimetry (DTG) of (a) blank microcapsules and (b) Imm-MC

Increased mass loss at low and intermediate temperatures confirms successful vitamin C incorporation and its thermal behavior within the matrix.

These results collectively demonstrate that EE and LC are controlled by the interplay between polymer network density, payload availability, and gelling duration. Vitamin C concentration runs the potential loading, while alginate concentration determines matrix structure and EE. Gelling time mainly affects stabilization and diffusion, but is less influential on LC. The models, validated by residual analysis and 3D response surfaces, provide a reliable framework for optimizing formulations to achieve high EE and acceptable LC for oral or aquatic delivery applications.

4. CONCLUSIONS

The study demonstrated that alginate concentration, vitamin C concentration, and gelling time significantly influence the EE and LC of vitamin C microcapsules. Optimal conditions (0.766% alginate, 59.36 ppm vitamin C, 1.81 min gelling time) achieved EE = 84.06% and LC = 0.47%, reflecting the effectiveness of response surface methodology for formulation optimization. SEM–EDS and thermal analyses confirmed successful incorporation of vitamin C within a calcium-crosslinked polymer matrix, with minimal structural defects and enhanced thermal stability. These findings provide a robust approach for developing microcapsule-based delivery systems for sensitive bioactive compounds.

ACKNOWLEDGMENT

This work is supported by the Philippine Department of Agriculture – National Fisheries Research and Development Institute (DA-NFRDI) under the Hatchery Production (HatchPro) Program, through the project titled “Increasing Innate and Adaptive Immunity Against Bacterial Pathogen of Nile Tilapia Using Immunostimulant and Vaccine-Loaded Microcapsules Using Biopolymer as a Potential Application for Immunobooster and Oral Vaccination”.

REFERENCES

[1] Carr, A.C., Maggini, S. (2017). Vitamin C and immune function. Nutrients, 9(11): 1211. https://doi.org/10.3390/nu9111211

[2] Vijayaram, S., Ringø, E., Zuorro, A., van Doan, H., Sun, Y. (2024). Beneficial roles of nutrients as immunostimulants in aquaculture: A review. Aquaculture and Fisheries, 9(5): 707-720. https://doi.org/10.1016/j.aaf.2023.02.001

[3] Omoniyi, A.D., Ovie, I.A. (2018). Vitamin C: An important nutritional factor in fish diets. Journal of Agriculture and Ecology Research International, 16(2): 1-7. https://doi.org/10.9734/JAERI/2018/15528

[4] Mieszczakowska-Frąc, M., Celejewska, K., Płocharski, W. (2021). Impact of innovative technologies on the content of vitamin C and its bioavailability from processed fruit and vegetable products. Antioxidants, 10(1): 54. https://doi.org/10.3390/antiox10010054

[5] Yin, X., Chen, K., Cheng, H., Chen, X., Feng, S., Song, Y., Liang, L. (2022). Chemical stability of ascorbic acid integrated into commercial products: A review on bioactivity and delivery technology. Antioxidants, 11(1): 153. https://doi.org/10.3390/antiox11010153

[6] Galindo-Villegas, J., Mulero, I., García-Alcazar, A., Muñoz, I., Peñalver-Mellado, M., Streitenberger, S., Mulero, V. (2013). Recombinant TNFα as oral vaccine adjuvant protects European sea bass against vibriosis: Insights into the role of the CCL25/CCR9 axis. Fish & Shellfish Immunology, 35(4): 1260-1271. https://doi.org/10.1016/j.fsi.2013.07.046

[7] Gudding, R., Lillehaug, A., Evensen, Ø. (1999). Recent developments in fish vaccinology. Veterinary Immunology and Immunopathology, 72(1-2): 203-212. https://doi.org/10.1016/S0165-2427(99)00133-6

[8] Bøgwald, J., Dalmo, R.A. (2019). Review on immersion vaccines for fish: An update 2019. Microorganisms, 7(12): 627. https://doi.org/10.3390/microorganisms7120627

[9] De, S., Robinson, D. (2003). Polymer relationships during preparation of chitosan–alginate and poly-l-lysine–alginate nanospheres. Journal of Controlled Release, 89(1): 101-112. https://doi.org/10.1016/S0168-3659(03)00098-1

[10] Neutra, M.R., Kozlowski, P.A. (2006). Mucosal vaccines: The promise and the challenge. Nature Reviews Immunology, 6(2): 148-158.

https://doi.org/10.1038/nri1777
[11] Klojdová, I., Milota, T., Smetanová, J., Stathopoulos, C. (2023). Encapsulation: A strategy to deliver therapeutics and bioactive compounds? Pharmaceuticals, 16(3): 362. https://doi.org/10.3390/ph16030362
[12] Gagelonia, J.D., Marfil, M.L.M., Velasco, R.R., Suyom, J.C. (2024). Feed maximization of combined culture of Nile tilapia Oreochromis niloticus and African catfish Clarias gariepinus. Aquaculture, Aquarium, Conservation & Legislation, 17(1): 352-359.
[13] Abourehab, M.A., Rajendran, R.R., Singh, A., Pramanik, S., Shrivastav, P., Ansari, M.J., Deepak, A. (2022). Alginate as a promising biopolymer in drug delivery and wound healing: A review of the state-of-the-art. International Journal of Molecular Sciences, 23(16): 9035. https://doi.org/10.3390/ijms23169035
[14] Noor-ul-Ain, R., Ilyas, N., Saeed, M., Subramaniam, G., Mastinu, A. (2025). Advances in pharmaceutical and biomedical applications of plant–based nano-biopolymers with special emphasis on vaginal drug delivery systems: A review. Industrial Crops and Products, 225: 120592. https://doi.org/10.1016/j.indcrop.2025.120592
[15] Wang, H., Wang, S., Fang, R., Li, X., Xing, J., Li, Z., Song, N. (2023). Enhancing TB vaccine efficacy: Current progress on vaccines, adjuvants and immunization strategies. Vaccines, 12(1): 38. https://doi.org/10.3390/vaccines12010038
[16] Saberian, M., Roudsari, R.S., Haghshenas, N., Rousta, A., Alizadeh, S. (2024). How the combination of alginate and chitosan can fabricate a hydrogel with favorable properties for wound healing. Heliyon, 10(11): e32040. https://doi.org/10.1016/j.heliyon.2024.e32040
[17] Choudhury, N., Meghwal, M., Das, K. (2021). Microencapsulation: An overview on concepts, methods, properties and applications in foods. Food Frontiers, 2(4): 426-442. https://doi.org/10.1002/fft2.94
[18] Arun, J.K., Vodeti, R., Shrivastava, B., Bakshi, V. (2020). Integrated quality by design approach for developing nanolipidic drug delivery systems of olmesartan medoxomil with enhanced antihypertensive action. Advanced Pharmaceutical Bulletin, 10(3): 379-388. https://doi.org/10.34172/apb.2020.046
[19] Chen, Z., Wei, W., Ni, B.J. (2022). Algae-based alginate biomaterial: Production and applications. In Biomass, Biofuels, and Biochemicals, pp. 37-66. https://doi.org/10.1016/B978-0-323-96142-4.00004-X
[20] Sultana, M., Chan, E.S., Pushpamalar, J., Choo, W.S. (2022). Advances in extrusion-dripping encapsulation of probiotics and omega-3 rich oils. Trends in Food Science & Technology, 123: 69-86. https://doi.org/10.1016/j.tifs.2022.03.006
[21] Pacharzina, I. (2025). Calibration curves: Creation and use. Anvajo. https://anvajo.com/inspiration/how-are-calibration-curves-created-and-what-information-can-they-provide.
[22] Drioli, E., Giorno, L. (2016). Encyclopedia of Membranes. Berlin: Springer Berlin Heidelberg. https://doi.org/10.1007/978-3-662-44324-8
[23] Yekdane, N., Goli, S.A.H. (2019). Effect of pomegranate juice on characteristics and oxidative stability of microencapsulated pomegranate seed oil using spray drying. Food and Bioprocess Technology, 12(9): 1614-1625. https://doi.org/10.1007/s11947-019-02325-8
[24] Piacentini, E. (2016). Encapsulation efficiency. In Encyclopedia of Membranes, pp. 706-707. https://doi.org/10.1007/978-3-662-44324-8_1945
[25] Al-Qadi, S., Grenha, A., Carrión-Recio, D., Seijo, B., Remuñán-López, C. (2012). Microencapsulated chitosan nanoparticles for pulmonary protein delivery: In vivo evaluation of insulin-loaded formulations. Journal of Controlled Release, 157(3): 383-390. https://doi.org/10.1016/j.jconrel.2011.08.008
[26] Doronio, J.P., Salazar, J.R., Monserate, J.J., Arevalo, B.J.A., Eugenio, P.J.G., Sarong, M.M. (2022). Nanoencapsulation of anthocyanin extract from fermented black garlic (FBG) based on biocompatible polymeric materials. Annales de Chimie Science des Matériaux, 46(1): 37-43. https://doi.org/10.18280/acsm.460105
[27] Xin, W., Wang, Y., Guo, X., Gou, K., Li, J., Li, S., Li, H. (2020). Biomimetic synthesis and evaluation of interconnected bimodal mesostructured MSF@ poly (Ethyleneimine) s for improved drug loading and oral adsorption of the poorly water-soluble drug, Ibuprofen. International Journal of Nanomedicine, 15: 7451-7468. https://doi.org/https://doi.org/10.2147/IJN.S272796
[28] Segale, L., Giovannelli, L., Mannina, P., Pattarino, F. (2016). Calcium alginate and calcium alginate-chitosan beads containing celecoxib solubilized in a self-emulsifying phase. Scientifica, 2016(1): 5062706. https://doi.org/10.1155/2016/5062706
[29] Bustos, D., Guzmán, L., Valdés, O., Muñoz-Vera, M., Morales-Quintana, L., Castro, R.I. (2023). Development and evaluation of cross-linked alginate–chitosan–abscisic acid blend gel. Polymers, 15(15): 3217. https://doi.org/10.3390/polym15153217
[30] Yulia, M., Rahmi, M., Hilmarni, H. (2023). Determination of vitamin C (ascorbic acid) content from orange fruit (Citrus reticulata Blanco) based on temperature and storage time. Asian Journal of Pharmaceutical Research and Development, 11(2): 6-8. https://doi.org/10.22270/ajprd.v11i2.1240
[31] Harvey, A., Palumbo, D. (2023). Score-driven models for realized volatility. Journal of Econometrics, 237(2): 105448. https://doi.org/10.1016/j.jeconom.2023.01.029
[32] Rousseaux, C.G., Gad, S.C. (2013). Statistical assessment of toxicologic pathology studies. Haschek and Rousseaux's Handbook of Toxicologic Pathology, 2: 893-988. https://doi.org/10.1016/B978-0-12-415759-0.00030-3
[33] Procopio, A., Lagreca, E., Jamaledin, R., La Manna, S., Corrado, B., Di Natale, C., Onesto, V. (2022). Recent fabrication methods to produce polymer-based drug delivery matrices (experimental and in silico approaches). Pharmaceutics, 14(4): 872. https://doi.org/10.3390/pharmaceutics14040872
[34] Rezagholizade-Shirvan, A., Soltani, M., Shokri, S., Radfar, R., Arab, M., Shamloo, E. (2024). Bioactive compound encapsulation: Characteristics, applications in food systems, and implications for human health. Food Chemistry: X, 24: 101953. https://doi.org/10.1016/j.fochx.2024.101953
[35] Gadziński, P., Froelich, A., Jadach, B., Wojtyłko, M., Tatarek, A., Białek, A., Osmałek, T. (2023). Ionotropic gelation and chemical crosslinking as methods for fabrication of modified-release gellan gum-based drug delivery systems. Pharmaceutics, 15(1): 108.

https://doi.org/10.3390/pharmaceutics15010108
[36] Gong, Y., Xiao, S., Yao, Z., Deng, H., Chen, X., Yang, T. (2024). Factors and modification techniques enhancing starch gel structure and their applications in foods: A review. Food Chemistry: X, 24: 102045. https://doi.org/10.1016/j.fochx.2024.102045
[37] Hicks, J., Dewey, J., Brandvain, Y., Schuchardt, A. (2020). Development of the biological variation in experimental design and analysis (BioVEDA) assessment. PloS One, 15(7): e0236098. https://doi.org/10.1371/journal.pone.0236098
[38] Venkatachalam, K., Charoenphun, N., Nitikornwarakul, C., Lekjing, S. (2025). Effect of sodium alginate concentration on the physicochemical, structural, functional attributes, and consumer acceptability of gel beads encapsulating tangerine peel (Citrus reticulata Blanco 'Cho Khun') extract. Gels, 11(10): 808. https://doi.org/10.3390/gels11100808
[39] Higazy, M.G. (2019). Analysis and accuracy of experimental methods. International Journal of Petrochemistry and Research, 3: 262-268. https://doi.org/10.18689/ijpr-1000145
[40] Li, C., Wang, Z.Y., He, Z.J., Li, Y.J., Mao, J., Dai, K.H., Zheng, J.C. (2021). An advance review of solid-state battery: Challenges, progress and prospects. Sustainable Materials and Technologies, 29: e00297. https://doi.org/10.1016/j.susmat.2021.e00297
[41] Gandham, V.D., Brochu, A.B., Reichert, W.M. (2012). Microencapsulation of liquid cyanoacrylate via in situ polymerization for self-healing bone cement application. MRS Online Proceedings Library (OPL), 1417: mrsf11-1417-kk01-06. https://doi.org/10.1557/opl.2012.1014
[42] Sauce-Guevara, M.A., García-Schejtman, S.D., Alarcon, E.I., Bernal-Chavez, S.A., Mendez-Rojas, M.A. (2025). Development and characterization of an injectable alginate/chitosan composite hydrogel reinforced with cyclic-RGD functionalized graphene oxide for potential tissue regeneration applications. Pharmaceuticals, 18(5): 616. https://doi.org/10.3390/ph18050616

NOMENCLATURE

ft	Foot, equivalent to 12 inches
min	Minutes, equivalent to 60 seconds
nm	Absorbance reading refers to the wavelength (in nanometers) of light at which the absorbance of a sample is measured.
R^2	Coefficient of determination
w/w	Weight of concentration in a solution, %
w/v	Mass of solute in a solution, %
v/v	Volume of concentration in solution, %

Greek symbols

$\pi \rightarrow \pi^*$	Pi to pi-star refers to a type of electronic transition in a molecule, particularly in molecular orbital theory and UV–Visible spectroscopy
λmax	Lambda max represents the highest or peak wavelength in the spectrophotometer reading

Subscripts

2	+2 charge of the single ion